The FEBS Journal

FEBS PRESS science publishing by scientists

Transcriptional factor ISL1 regulates palate development by tuning the SHH cascade

Chujing Zhang, Yuting Zheng, Yaping Qu, Ruiqi Huang, Huarong Huang, Jianying Li, Mengsheng Qiu and Feixue Li

Zhejiang Key Laboratory of Organ Development and Regeneration, Institute of Developmental and Regenerative Biology, College of Life and Environmental Sciences, Hangzhou Normal University, China

Keywords
cleft palate; epithelial–mesenchymal interaction; Isl1; Shh; signal pathway

Correspondence
F. Li, Zhejiang Key Laboratory of Organ Development and Regeneration, Institute of Developmental and Regenerative Biology, College of Life and Environmental Sciences, Hangzhou Normal University, Hangzhou 310036, China
Tel: +86 571 28865657
E-mail: lifx@hznu.edu.cn

Chujing Zhang and Yuting Zheng contributed equally to this article.

(Received 1 February 2024, revised 31 August 2024, accepted 12 December 2024)

doi:10.1111/febs.17369

Cleft palate is one of the most common birth defects in humans, and palate morphogenesis depends on epithelial–mesenchymal interaction. In this study, we report that ablation of *Isl1* in the epithelium leads to complete cleft palate. A significant reduction in mesenchymal cell proliferation was detected in the $Isl1^{Pitx2Cre}$ mutant palates, but there was no significant difference in apoptosis between wild-type and mutant embryos. Fewer rugae structures were observed in $Isl1^{Pitx2Cre}$ mutant embryos. *Shh*, *Sox2*, *Foxe1*, *Foxd2*, and *Msx1* expression was downregulated in the developing palate in *Isl1* mutant embryos. We found that ISL1 can directly regulate *Shh* expression in palatal epithelial cells, suggesting a critical role for ISL1 in epithelial–mesenchymal interactions during palate development. Remarkably, cleft palate defects due to *Isl1* deletion were rescued by a conditional transgenic allele (Tg-*pmes-Ihh*), confirming the genetic integration of Hedgehog signaling. Our findings indicate that ISL1 controls palatal shelf morphogenesis by modulating epithelial-mesenchymal communication via SHH signaling.

Introduction

Cleft lip and/or cleft palate are common craniofacial anomalies, occurring in approximately 1 in 700 newborns [1–4]. The palate forms through the fusion of the primary and secondary palates. The primary palate, developed from the medial frontonasal processes, forms the premaxillary region. The secondary palate, which originates from the maxillary process, contributes to the development of the hard and soft parts of the palate [5]. In mice, palatogenesis begins at embryonic day 11.5 (E11.5). The bilateral maxillary prominences extend into the oral cavity to form a pair of palatal shelves, which grow vertically downward from the lingual side during E12.5–E13.5. Around E14.0, the palatal shelves elevate to a horizontal position above the tongue and subsequently adhere and fuse medially to form the secondary palate. The anterior two-thirds of the palate ossify to form the hard palate, while the posterior one-third forms the soft palate.

The palate consists mainly of oral epithelium and neural crest cell-derived mesenchyme. Epithelial–mesenchymal interactions play a pivotal role in developing the secondary palate [6–8]. *Shh*, expressed in epithelial cells, is an early key signaling molecule in palate development [9]. Its expression is highly

Abbreviations
BrdU, bromodeoxyuridine; ChIP, chromatin immunoprecipitation; Foxd2, forkhead box D2; Foxe1, forkhead box E1; Ihh, Indian hedgehog; Isl1, insulin enhancer binding protein-1; MEE, medial edge epithelium; Msx1, Msh homeobox 1; RNA-Seq, RNA sequencing; Shh, Sonic hedgehog; Smo, smoothened; Sox2, SRY-box transcription factor 2; TUNEL, terminal deoxynucleotidyl transferase (TdT) dUTP nick-end labeling.

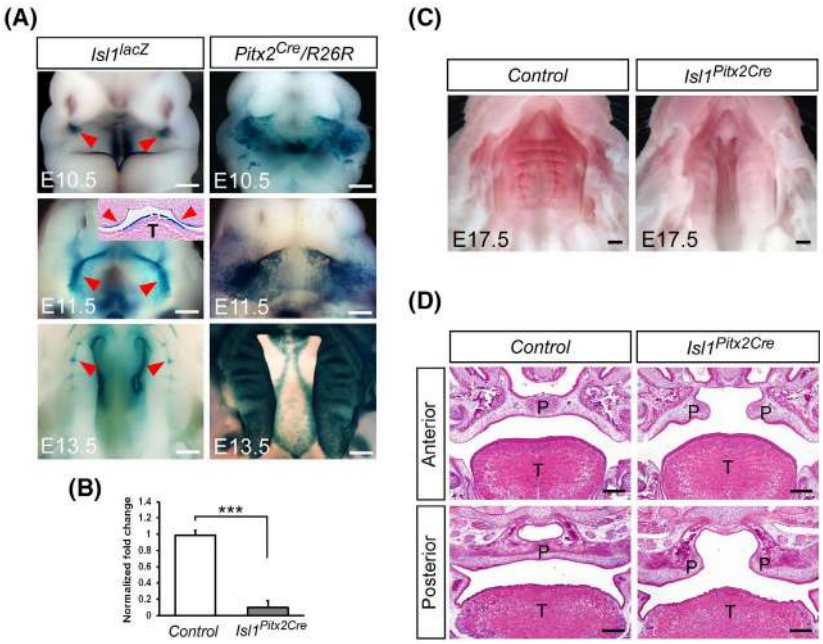

Fig. 1. Epithelial specific inactivation of *Isl1* leads to cleft palate. (A) X-Gal staining showing *Isl1* expression in $Isl1^{LacZ}$ knock-in mice at E10.5, E11.5, and E13.5 (red arrowheads) (left panel) ($n = 4$). X-Gal staining showing Pitx2-Cre activity in $Pitx2^{Cre}/R26R$ mice at E10.5, E11.5, and E13.5 (right panel) ($n = 4$). (B) Quantitative real-time PCR demonstrated transcription of *Isl1* in the $Pitx2^{Cre}$ (Control) and $Isl1^{Pitx2Cre}$ palates at E12.5 ($n = 5$). Student's *t*-test was used to test differences between Control and $Isl1^{Pitx2Cre}$. (C) Oral view of the palate in control ($Pitx2^{Cre}$) and $Isl1^{Pitx2Cre}$ mice at E17.5 ($n = 4$). (D) Representative frontal sections from the anterior and posterior regions of the developing palatal shelves in control ($Pitx2^{Cre}$) and $Isl1^{Pitx2Cre}$ at E17.5 ($n = 4$). Error bars represent standard deviations. $***P < 0.001$. Scale bars, 200 μm (A); 500 μm (C, D). P, palatal shelf; T, tongue.

restricted to the thickened palatal rugae epithelium regions, which act as signaling centers that regulate palatogenesis [10–13]. Epithelial-specific knockdown of *Shh* gene or mesenchymal-specific inactivation of *Smo* gene leads to palate growth defects [14]. Additionally, treatment with 5E1, an anti-SHH antibody, delays rugae placode formation and disrupts cell proliferation [11]. Numerous transcription factors are involved in palate development, including *Sox2* and *Foxe1* [15–17]. *Sox2* is implicated in rugae formation and palate development, while *Foxe1* has been associated with isolated cleft lip with or without cleft palate and isolated cleft palate [15,16]. MSX1 is critical for anterior palatal mesenchyme proliferation, and *Msx1*-deficient mice exhibit complete cleft of the secondary palate [17].

ISL1, a member of the LIM homeodomain transcription factor family, plays key roles in various organs during embryonic development, such as the limb, tongue, and heart [18–21]. The enhancer HS586, which regulates Isl1 expression, is linked to normal facial morphology and craniofacial birth defects [22]. However, the exact role of Isl1 in rugae formation and palate development remains unclear. Here, we found that Isl1 ablation in the palate epithelium results in defects in rugae formation and cleft palate. Our data suggest that Isl1 regulates palate development through SHH signaling.

Results

Isl1 mutant mice exhibit complete cleft of the secondary palate

The expression of *Isl1* in the palate was determined using the $Isl1^{LacZ}$ knock-in allele, with Isl1 expression detected in the maxillary process as early as E10.5 (Fig. 1A). *Isl1* was expressed in the epithelium of palatal tissue folds at E11.5, when palatogenesis begins, and remained expression in the palate at E13.5 (Fig. 1A). To investigate the potential function of *Isl1* in palate development, we generated mice with epithelial cell-specific deletion of *Isl1* by crossing $Pitx2^{Cre}$ with $Isl1^{fl}$ mice ($Isl1^{Pitx2Cre}$). $Pitx2^{Cre}$ mice exhibited Cre activities in the maxillary epithelium at E10.5 and E11.5, and the palatal epithelium at E13.5 (Fig. 1A). The real-time PCR results showed that *Isl1* expression was significantly decreased in the palatal shelves of

Isl1^{Pitx2Cre} mutant mice at E12.5 (Fig. 1B). Mice heterozygous for the *Isl1* mutation appeared normal and fertile, whereas *Isl1*^{Pitx2Cre} mutant alleles displayed a complete cleft of the secondary palate with 100% penetration (Fig. 1C,D). Detailed histological analysis showed that the mutated palatal shelves had similar vertical positions on both sides of the tongue at E13.5 (Fig. 2). At E14.5, the mutant embryos' shelves elevated normally to the horizontal position above the tongue (Fig. 2). By E15.5, the mutant palatal shelves remained separated from each other (Fig. 2). These results suggest that *Isl1* deficiency hindered the palatal shelves outgrowth but not elevation.

Loss of Isl1 does not disrupt fusion of palatal shelves

To assess whether the fusion competency of palatal shelves was altered in the mutant, *in vitro* organ culture experiments were conducted. The bilateral palatal shelves were cultured with the medial edge epithelium (MEE) in contact. The *in vitro* data indicated that *Isl1*^{Pitx2Cre} palatal shelves retain their ability to fuse, supporting the hypothesis that the cleft secondary palate in the mutant embryos results from a failure of palatal shelf growth (Fig. 3A). This conclusion was further supported by positive TUNEL staining in the medial portion of the palatal shelf at E14.5 in the mutant, coinciding with apoptosis in the midline seam in wild-type controls (Fig. 3B). Additionally, skeletal staining of *Isl1* mutants revealed widely separated palatal shelves (Fig. 3C). These data suggest that *Isl1* deletion does not alter the fusion competency of palatal shelves.

Isl1 deletion leads to defective palate shelf growth

To understand the cellular mechanisms underlying cleft palate in *Isl1* mutants, we examined cell proliferation using BrdU labeling. Immunofluorescence results showed a significant reduction in BrdU-labeled mesenchymal cells in the anterior palate region, but not in the posterior palate region, of *Isl1*^{Pitx2Cre} embryos at E13.5 compared with wild-type controls (Fig. 4A,B). TUNEL assays on E13.5 tissue sections revealed no significant difference in apoptosis between wild-type (*Pitx2*^{Cre}) and *Isl1*^{Pitx2Cre} embryos (Fig. 4C). These results suggest that *Isl1* is critical for cell proliferation during palate development but not for cell survival. The reduction in palatal cell proliferation may account for the cleft palate pathogenesis observed in *Isl1* mutant mice.

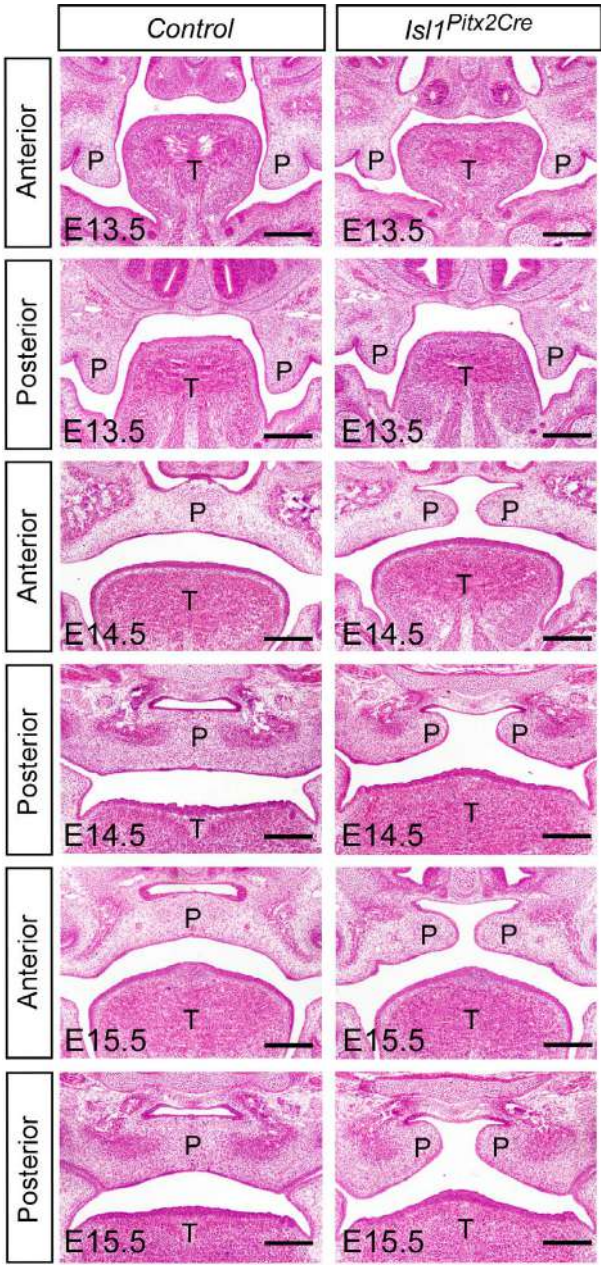

Fig. 2. Histological analysis of palate developmental defects in *Isl1*^{Pitx2Cre} mutant embryos. Representative frontal sections from the anterior and posterior regions of the developing palatal shelves in control (*Pitx2*^{Cre}) and *Isl1*^{Pitx2Cre} at E13.5-E15.5 ($n = 5$). P, palatal shelf; T, tongue. Scale bars, 200 μm.

Isl1 is required for rugae development

To explore the molecular mechanisms by which *Isl1* deletion causes cleft palate, we analyzed gene expression profiles via RNA-Seq using RNA extracted from E12.5 palate shelves from mutant (*Isl1*^{Pitx2Cre}) and control (*Pitx2*^{Cre}) embryos. Comparative analysis uncovered

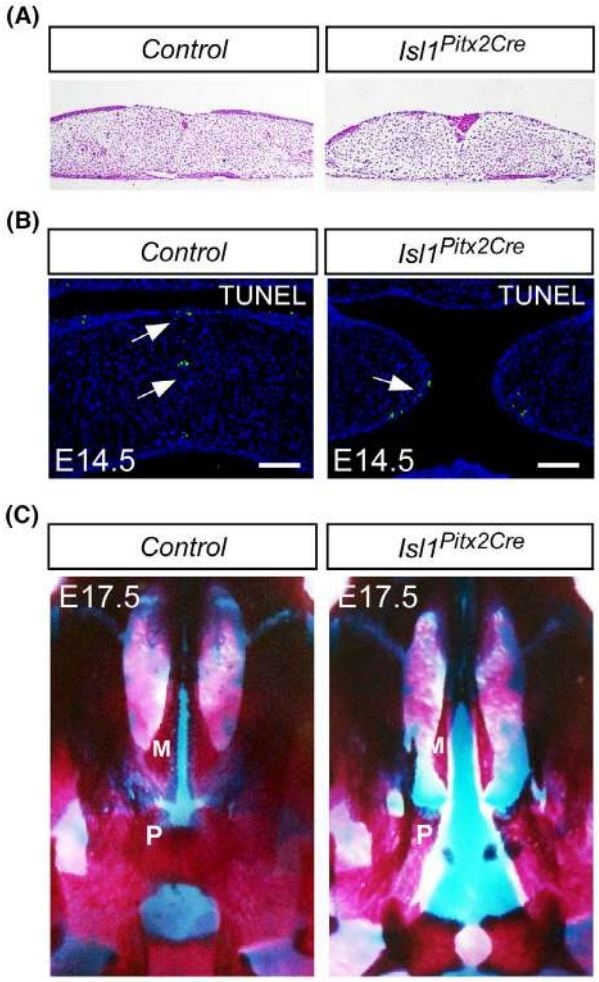

Fig. 3. Fusion of palatal shelves is not impaired in *Isl1*^{Pitx2Cre} mice. (A) The palatal shelves of E13.5 *Isl1*^{Pitx2Cre} mutant embryos fused as well as those of wild-type control embryos *in vitro* ($n = 3$). (B) TUNEL assay showed cell apoptosis of palate from E14.5 control and *Isl1*^{Pitx2Cre} embryos (arrows) ($n = 4$). (C) Skeletal preparation of E17.5 wild-type embryo and *Isl1*^{Pitx2Cre} mutant palates. Unlike normally closed palatine shelves in wild-type, palatine shelves are widely-separated in *Isl1*^{Pitx2Cre} mutants ($n = 3$). M, maxillary shelf; P, palatal shelf. Scale bars, 100 μm.

dozens of differentially expressed protein-coding genes in the mutant versus the control (≥ 1.5 fold, < 5% false discovery rate) (Fig. 5A). Gene ontology (GO) term analyses revealed that multicellular organism development, pattern specification process, and signal transduction involved in regulation of gene expression were significantly affected (Fig. 5B). The expression of *Shh* and *Sox2*, which play key roles in signal transduction and pattern specification, is significantly downregulated [14,16]. Both SHH signaling and *Sox2* are essential for palatal shelf extension and rugae formation, which are signaling centers that regulate palatogenesis. We

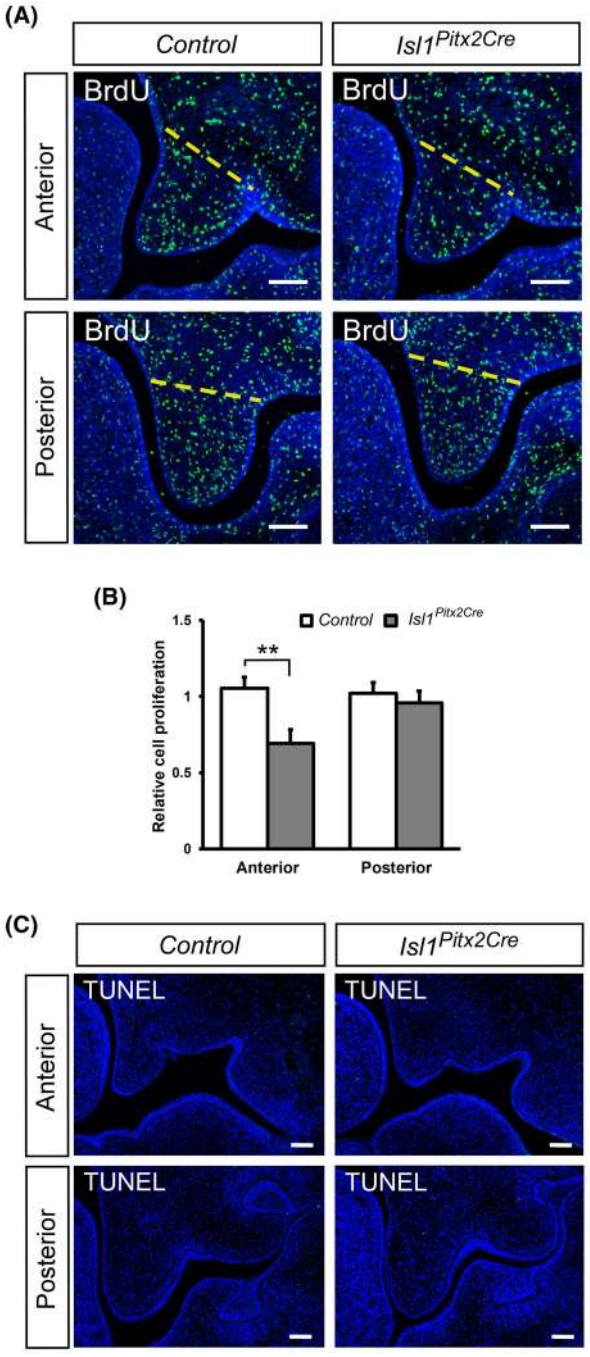

Fig. 4. Aberrant cell proliferation in the palatal shelf of *Isl1*^{Pitx2Cre} mice. (A) BrdU labeling assays showed that the level of cell proliferation in the anterior palate of E13.5 *Isl1*^{Pitx2Cre} embryo was lower than that in the control (*Pitx2*^{Cre}) ($n = 5$). Yellow dotted lines delineates the palatal region for counting of BrdU-labeled cells. (B) Comparison of relative proliferation of BrdU-labeled cells between control and *Isl1*^{Pitx2Cre} embryo palatal mesenchyme ($n = 5$). Student's *t*-test was used to test differences between Control and *Isl1*^{Pitx2Cre}. (C) TUNEL staining in the anterior and posterior regions of E13.5 palates in *Pitx2*^{Cre} (Control) and *Isl1*^{Pitx2Cre} mice ($n = 5$). Error bars represent standard deviations. $^{**}P < 0.01$. Scale bars, 100 μm.

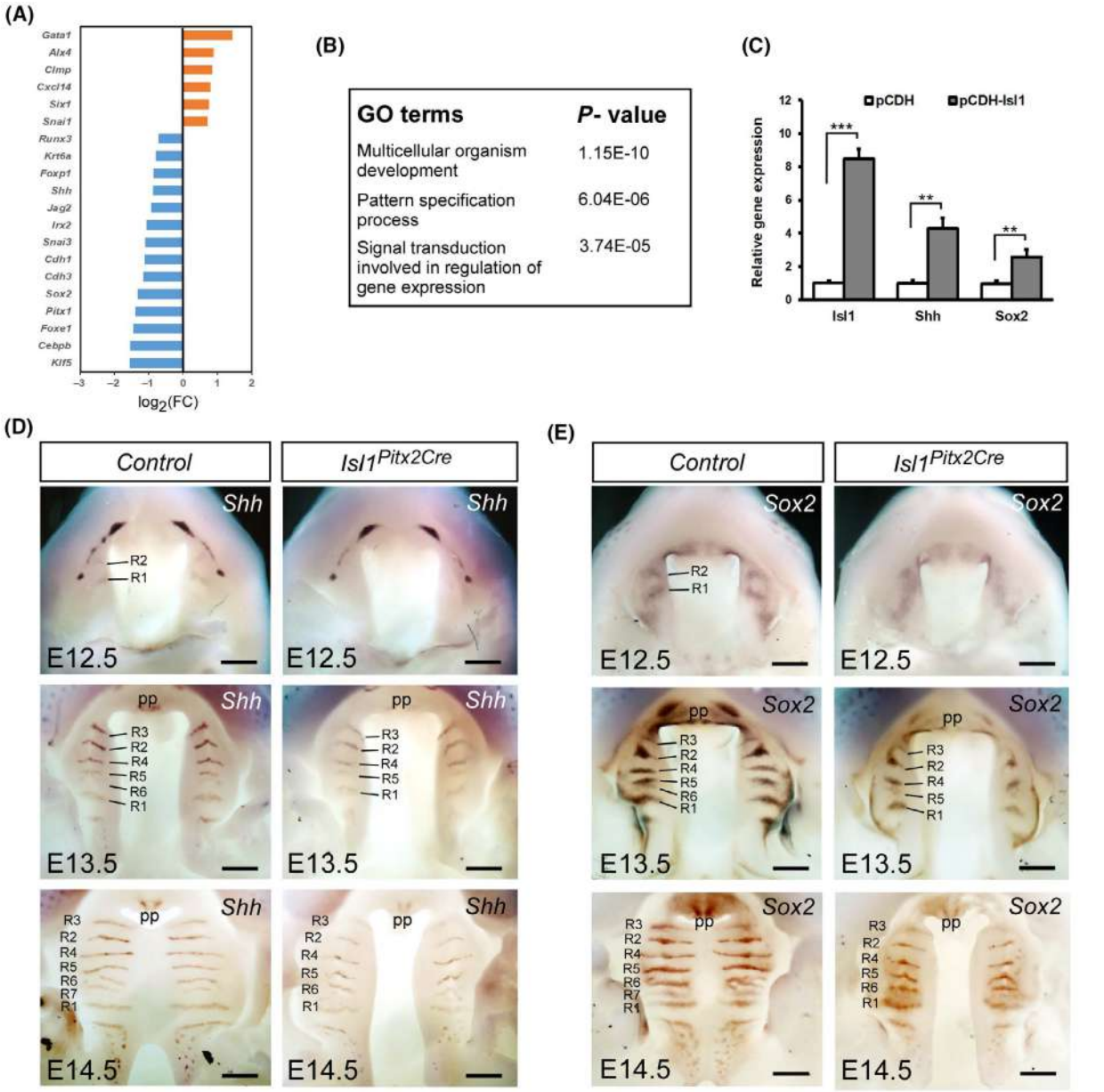

Fig. 5. Palatal *Shh* and *Sox2* mRNA expression pattern in *Isl1*^{Pitx2Cre} mutant embryos. (A) Representative examples of differentially expressed genes in the *Isl1*^{Pitx2Cre} as revealed by RNA-Seq analysis (≥ 1.5-fold, < 5% false discovery rate). (B) Gene ontology (GO) term analyses identified the significantly affected biological processes. (C) Quantitative real-time PCR demonstrated transcription of *Isl1*, *Sox2* and *Shh* in palate cultures ($n = 6$). *Isl1* overexpression vector (pCDH-Isl1) or control vector (pCDH) was transfected into explants with Lipofectamine 3000 reagent. Student's *t*-test was used to test differences between pCDH and pCDH-Isl1. (D) Whole-mount *in situ* hybridization showed the expression of *Shh* in the *Pitx2*^{Cre} (Control) and *Isl1*^{Pitx2Cre} palates at E12.5-E14.5 ($n = 5$). R1–R7 marks the individual rugae in the order in which it was formed. *Shh* labeled palatal rugae increased from two pairs at E12.5 to seven pairs at E14.5 in wild-type embryos, whereas mutants formed only six pairs at E14.5. (E) Whole-mount *in situ* hybridization showing the expression of *Sox2* in the *Pitx2*^{Cre} (Control) and *Isl1*^{Pitx2Cre} palates at E12.5–E14.5 ($n = 5$). In the mutant (*Isl1*^{Pitx2Cre}), only six pairs of *Sox2*-labeled palatal folds were formed at E14.5. pp, primary palate. Scale bars, 200 μm. Error bars represent standard deviations. $^{**}P < 0.01$, $^{***}P < 0.001$.

confirmed *Shh* and *Sox2* as downstream target genes of ISL1 using an *in vitro* palatal shelf culture system, where overexpression of *Isl1* in the *Isl1*^{Pitx2Cre} mutant palate significantly upregulated their expression (Fig. 5C). Whole-mount *in situ* hybridization showed decreased *Shh* and *Sox2* expression in mutant palate shelves at E12.5,

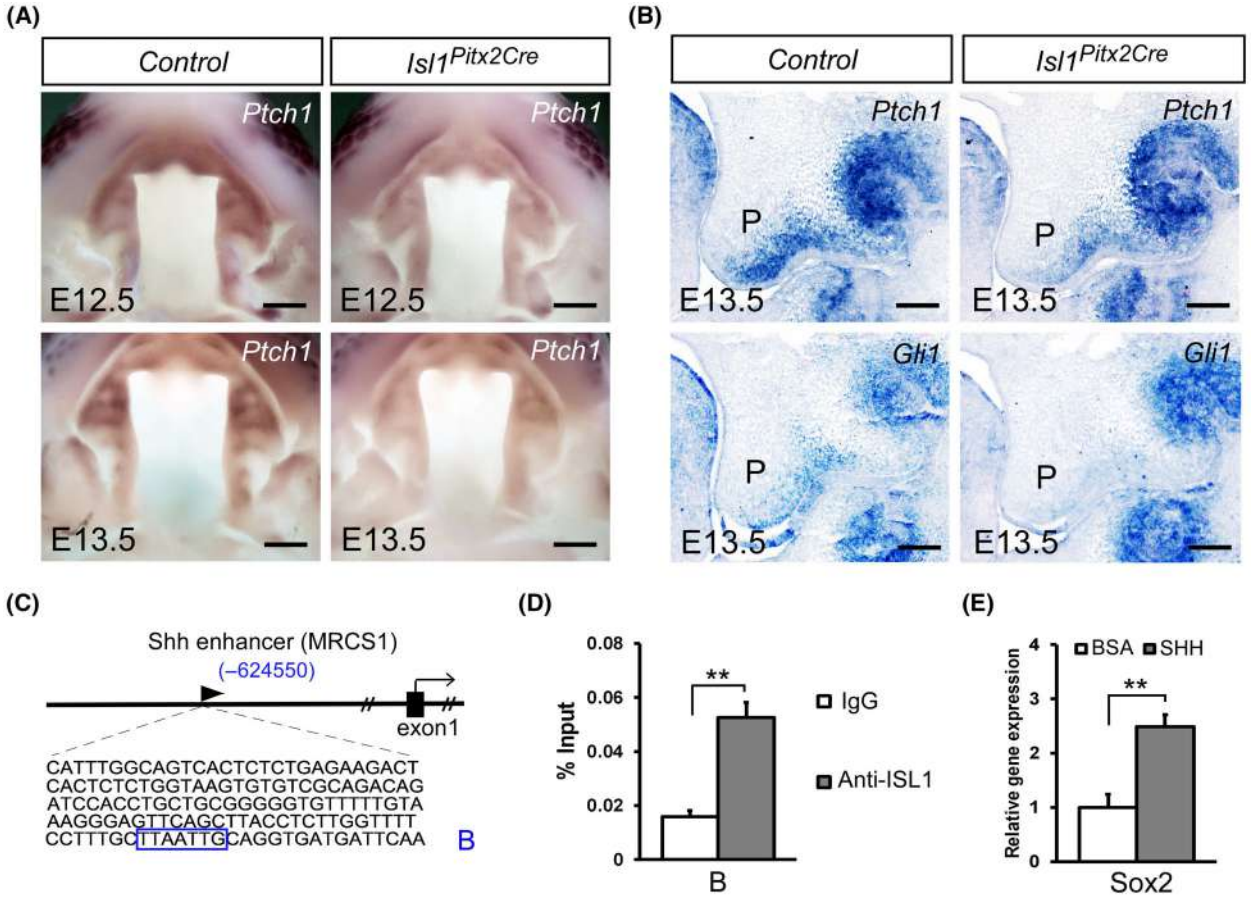

Fig. 6. *Isl1* sustains the Hedgehog pathway via regulation of *Shh* expression. (A) Whole-mount *in situ* hybridization showed the expression of *Ptch1* in the $Pitx2^{Cre}$ (Control) and $Isl1^{Pitx2Cre}$ palates at E12.5-E13.5 ($n = 5$). (B) *In situ* hybridization showed the expression of *Ptch1* and *Gli1* in the $Pitx2^{Cre}$ (Control) and $Isl1^{Pitx2Cre}$ palates at E13.5 ($n = 5$). (C) Schematic representation of the Shh epithelial enhancer sequence (MRCS1). The binding site for ISL1 was highlighted "B". (D) Quantitative analysis of ChIP assays was performed by real-time PCR ($n = 6$). Chromatin extracts were precipitated in the presence of nonspecific mouse IgG or antibody against ISL1 (Anti-ISL1). Student's *t*-test was used to test differences between IgG and Anti-ISL1. (E) Quantitative real-time PCR demonstrated transcription of *Sox2* after SHH treatment in palate cultures ($n = 6$). Student's *t*-test was used to test differences between BSA and SHH. Error bars represent standard deviations. $^{**}P < 0.01$. Scale bars, 200 μm (A); 100 μm (B). P, palatal shelf.

E13.5, and E14.5 (Fig. 5D,E). At E12.5, *Isl1* mutant embryos exhibited diffuse *Shh* and *Sox2* expression in the palatal epithelium and lacked well-defined rugae structures (Fig. 5D,E). From E12.5 to E14.5, *Shh* and *Sox2* expression remained weaker in the mutant palate compared to wild-type controls, with fewer *Shh*-expressing and *Sox2*-expressing rugae structures (Fig. 5D,E). The mutant embryos also showed reduced *Shh* and *Sox2* expression in the primary palate (Fig. 5D,E).

ISL1 regulates SHH signaling during palatal morphogenesis

Palatal morphogenesis involves critical interactions between the epithelium and mesenchyme. We hypothesized that the transcription factor ISL1, expressed in epithelial cells, regulates mesenchymal cell activity via the secreted signaling molecule SHH. To assess Hedgehog signaling activity in the mesenchyme of $Isl1^{Pitx2Cre}$ mutant palates, we performed *in situ* hybridization. Our results revealed a marked downregulation of *Ptch1* and *Gli1*, two key markers of active Hedgehog signaling, in $Isl1^{Pitx2Cre}$ mutants (Fig. 6A, B). Previous studies have shown that SHH expression in the palatal epithelium is controlled by the MRCS1 sequence [23]. Within this sequence, we identified a potential binding site for ISL1 (Fig. 6C). ChIP analysis further confirmed ISL1's ability to bind to this site (Fig. 6D). Additionally, SHH protein treatment significantly induced the expression of *Sox2* (Fig. 6E),

suggesting that SHH is a direct target of ISL1 and that *Sox2* expression is regulated by SHH.

Members of the Forkhead Box (Fox) transcription factor family, including *Foxe1* and *Foxd2*, have been identified as downstream targets of the SHH signaling pathway. Our data demonstrated that SHH stimulation robustly induced *Foxe1* and *Foxd2* expression (Fig. 7A). Mutations in *Foxe1* are known to cause Bamforth–Lazarus syndrome, a condition associated with cleft palate [15]. The *Msx1* gene, critical for epithelial–mesenchymal interactions during palate development, has been identified as a downstream target of FOXE1. Whole-mount *in situ* hybridization further revealed that the expression levels of *Foxe1*, *Foxd2*, and *Msx1* were significantly reduced in the palates of $Isl1^{Pitx2Cre}$ mutant embryos (Fig. 7B). These findings suggest that ISL1 influences palatal growth by modulating SHH signaling, which, in turn, regulates the expression of key downstream target genes.

Activation of Hedgehog signaling rescues palate morphogenesis defects *in vivo*

We further validated the hypothesis that ISL1 regulates palatal development through Hedgehog signaling by conditionally overexpressing IHH in palatal epithelial cells using a conditional transgenic allele (Tg-*pmes-Ihh*). IHH activates the same canonical Hedgehog signaling pathway as SHH [24]. Overexpression of *Ihh* in $Isl1^{Pitx2Cre}$; Tg-*pmes-Ihh* embryos successfully rescued the palatal morphogenesis defects observed in $Isl1^{Pitx2Cre}$ embryos (Fig. 8A). Additionally, the expression of *Ptch1* was significantly upregulated in the palate mesenchyme of $Isl1^{Pitx2Cre}$; Tg-*pmes-Ihh* compared to $Isl1^{Pitx2Cre}$ embryos (Fig. 8B), confirming that the transgenic IHH acted as a functional secreted ligand in the mesenchyme. The defect in cell proliferation was also rescued in $Isl1^{Pitx2Cre}$; Tg-*pmes-Ihh* embryos compared to $Isl1^{Pitx2Cre}$ embryos (Fig. 8C,D). These findings demonstrate that *Ihh* overexpression effectively restores palate development defects caused by *Isl1* deletion, further supporting the genetic interaction between *Isl1* and Hedgehog signaling in palatal morphogenesis.

Discussion

Numerous growth factors and signaling pathways play crucial roles in the growth, elevation, or fusion processes during palatogenesis [25–29]. In this study, our finding of cleft secondary palate defect in $Isl1^{Pitx2Cre}$ mutant embryos suggests the importance of ISL1 in palate development. Our findings demonstrate that cleft palate primarily results from a failure in palate growth. We provide evidence that SHH signaling mediates the regulatory effect of ISL1 on palate development.

Palatogenesis is a complex process involving the initiation, growth, morphogenesis, and fusion of the primary and secondary palatal shelves. *Isl1* is highly expressed in the epithelia of the maxillary process as early as E10.5, indicating its potential role in regulating palatal development. Complete cleft palate was observed following *Isl1* ablation in the palatal epithelium. The $Isl1^{Pitx2Cre}$ mutant palatal shelves exhibited normal elevation to a horizontal position above the tongue, suggesting that *Isl1* is not essential for palatal shelf elevation. Furthermore, the mutant palatal shelves could fuse in an *in vitro* organ culture, indicating that the fusion process was not affected by *Isl1* deletion. The shorter palatal shelves in mutants compared to wild-type suggest a defect in palatal shelf growth. Proper cell proliferation is essential for the normal growth of craniofacial structures, and our results showed a significantly reduction in cell proliferation in the anterior palate region of $Isl1^{Pitx2Cre}$ embryos.

In addition to defects in palatal growth, we also detected deficiency in palatal rugae formation following *Isl1* deletion. Previous studies have shown that *Shh* and *Sox2* mRNA are expressed in palatal rugae and follow a distinct temporal sequence during palatal growth [12,13,25]. SHH signaling in the palatal ridge ensures that the palate extends to the midline [30,31]. *Sox2* is required for formation palatal rugae, which serve as signaling centers that regulate palatogenesis [16]. Deletion of the *Sox2* gene in oral epithelium disrupts palatal rugae formation and palatal shelf extension [16]. Our *in situ* data for *Shh* and *Sox2* indicate impairments in palatal shelf growth in mutant embryos. The growth of palatal shelves is regulated by epithelial-mesenchymal interactions, suggesting a link between epithelial expressed ISL1 and secretory signaling molecules.

The secreted protein Sonic hedgehog (SHH) is a critical early signal driving palatal shelf growth [9]. Epithelial-specific inactivation of *Shh* and mesenchymal-specific inactivation of *Smo* indicate that SHH signaling promotes palatal cell proliferation and growth [14]. Additionally, exogenous SHH protein can stimulate palatal mesenchyme proliferation [32]. Our study shows that *Shh* is regulated by ISL1, consistent with previous reports that *Shh* is a target gene for ISL1 in the lung and urethral epithelium [33]. Our results indicate that *Shh* and *Ptch1* expression in the palate is reduced following *Isl1* deletion. Another ligand for the Hedgehog signaling pathway is IHH,

which plays an important role in bone and cartilage development and is expressed in cranial osteoblasts [34]. RNA-Seq revealed no difference in *Ihh* expression between wild-type and mutant palate shelves, and the expression of *Ihh* was very low. Although both IHH and SHH activate the canonical Hedgehog pathway,

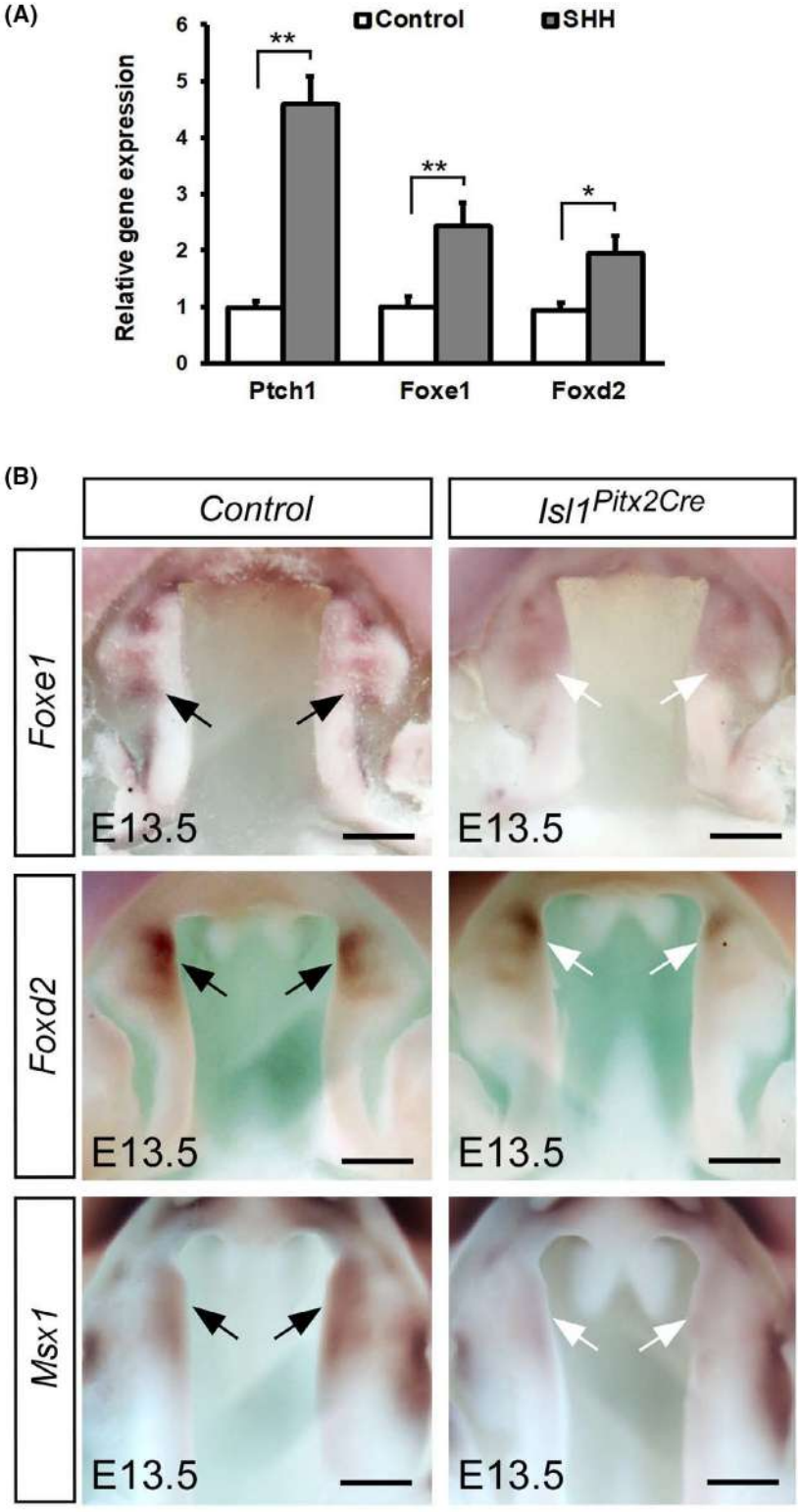

Fig. 7. Expression of *Foxe1*, *Foxd2* and *Msx1* mRNA expression in the palatal shelves. (A) Quantitative real-time PCR demonstrated transcription of *Ptch1*, *Foxe1* and *Foxd2* in palate organ cultures after SHH protein treatment ($n = 6$). Student's *t*-test was used to test differences between BSA and SHH. (B) Whole-mount *in situ* hybridization showed the expression of *Foxe1*, *Foxd2* and *Msx1* in the $Pitx2^{Cre}$ (Control) and $Isl1^{Pitx2Cre}$ palates at E13.5 ($n = 5$). Black arrows show the expression regions of *Foxe1*, *Foxd2* and *Msx1* in Control, while white arrows show the expression regions of *Foxe1*, *Foxd2* and *Msx1* in $Isl1^{Pitx2Cre}$. Error bars represent standard deviations. $^{*}P < 0.05$, $^{**}P < 0.01$. Scale bars, 200 μm.

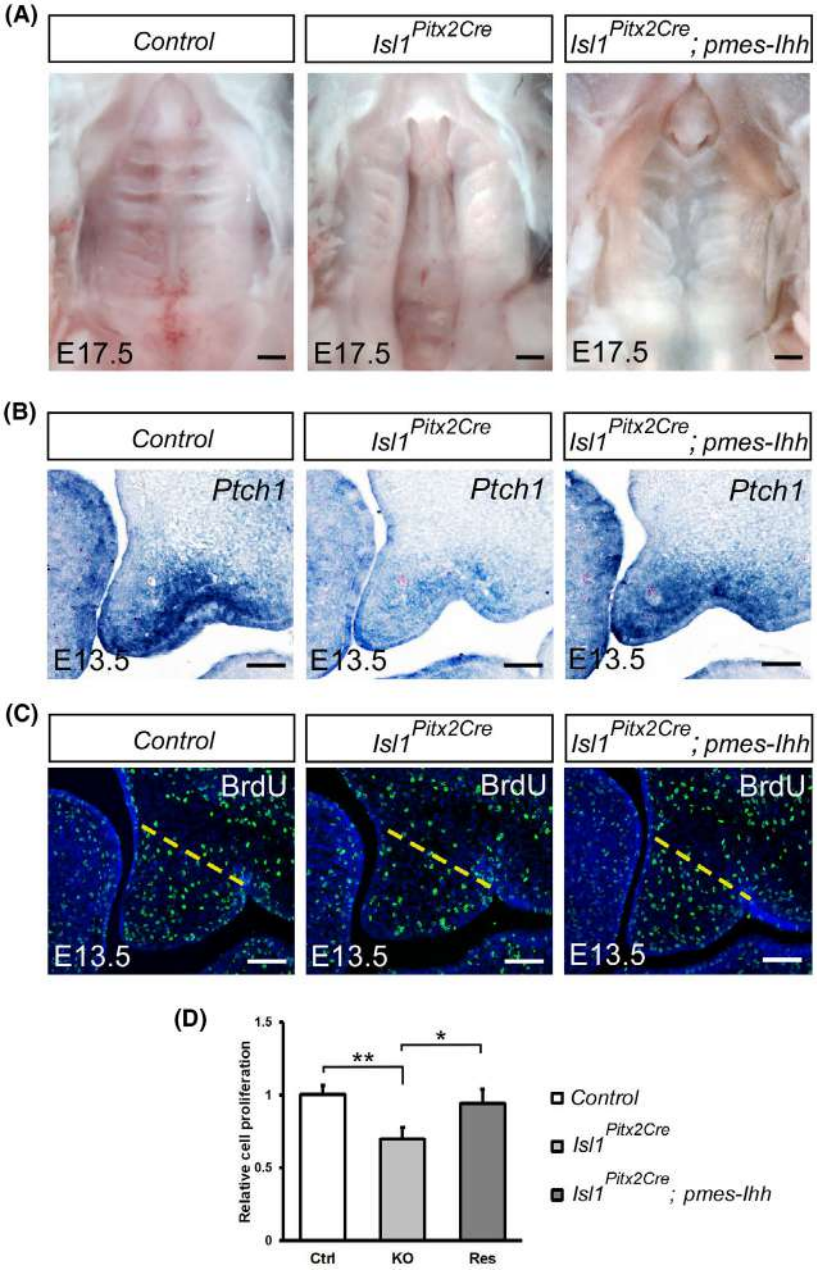

Fig. 8. Reactivation of Hedgehog signaling rescues cleft palate in $Isl1^{Pitx2Cre}$ mutant embryos. (A) Oral view of the palate in control ($Pitx2^{Cre}$), $Isl1^{Pitx2Cre}$, and $Isl1^{Pitx2Cre}$; Tg-*pmes-Ihh* embryos at E17.5 ($n = 5$). (B) *In situ* hybridization showed the expression of *Ptch1* in control ($Pitx2^{Cre}$), $Isl1^{Pitx2Cre}$, and $Isl1^{Pitx2Cre}$; Tg-*pmes-Ihh* embryos at E13.5 ($n = 5$). (C) BrdU labeling assays showed that the level of cell proliferation in the anterior palate of control ($Pitx2^{Cre}$), $Isl1^{Pitx2Cre}$, and $Isl1^{Pitx2Cre}$; Tg-*pmes-Ihh* embryos ($n = 5$). Yellow dotted lines delineates the palatal region for counting of BrdU-labeled cells. (D) Comparison of relative proliferation of BrdU-labeled cells between control ($Pitx2^{Cre}$), $Isl1^{Pitx2Cre}$, and $Isl1^{Pitx2Cre}$; Tg-*pmes-Ihh* palates ($n = 6$). One-way ANOVA and Tukey's test were used to analyze the difference between control ($Pitx2^{Cre}$), $Isl1^{Pitx2Cre}$, and $Isl1^{Pitx2Cre}$; Tg-*pmes-Ihh*. Error bars represent standard deviations. $^{*}P < 0.05$, $^{**}P < 0.01$. Scale bars, 500 μm (A); 100 μm (B, C).

they function in different tissues, and the activity of IHH ligands is much lower than SHH [35]. The activity of the Hedgehog signaling pathway is precisely regulated during palate development. Both loss-of-function and gain-of-function of Hedgehog signaling result in cleft palate [36]. Therefore, we overexpress

Ihh instead of *Shh* to avoid overactivation of the Hedgehog pathway. Overexpression of *Ihh* in palatal epithelium driven by Pitx2-Cre rescued the cleft palate phenotype and restored mesenchymal cell proliferation. IHH secreted by epithelial cells activates SMO and downstream signaling in mesenchymal cells in a paracrine manner to induce cell proliferation. The rescue experiments provide stronger evidence for the involvement of Hedgehog signaling pathway in palatal development.

Foxe1 and *Foxd2* have been reported as downstream target genes of SHH [37,38]. We demonstrated that SHH can induce the expression of *Foxe1* and *Foxd2* in the palate *in vitro*. Homozygous null mice with targeted disruption of *Foxe1* exhibited severe cleft palate, and *Msx1* has been identified as a downstream target of FOXE1 [17]. *Msx1* expression is almost absent in the palatal shelves of *Foxe1* mutant embryos. *Msx1* is essential for proper palate formation in humans and mice, with Msx1-deficient mice exhibiting complete cleft palate and cell proliferation defects in the anterior region [31]. *Msx1* expression was decreased in the palate of the $Isl1^{Pitx2Cre}$ embryos. These data suggest that the SHH signaling pathway mediates the effects of ISL1 on downstream target gene expression.

In summary, our data indicate that the transcriptional factor ISL1 is crucial for palate morphogenesis. The *Isl1* gene is critical for palatal shelf extension and rugae formation, and ISL1 is involved in regulating epithelial-mesenchymal interactions during palate development. Our findings suggest that Hedgehog signaling mediates the effects of ISL1 on palate development.

Materials and methods

Animals

All mouse experiments were conducted according to protocols approved by the Hangzhou Normal University Animal Care and Use Committee (2022-1057). The construction of *Isl1* conditional knockout allele ($Isl1^{fl}$) and *Isl1-lacZ* knock-in allele ($Isl1^{LacZ}$) has been described previously [39]. The conditional *Ihh* transgenic mice (Tg-*pmes-Ihh*) was constructed by inserting *Ihh* sequences into a site downstream of the LoxP-flanked STOP box controlled by the beta actin promoter [40]. *Pitx2* Cre knock-in allele ($Pitx2^{Cre}$) was purchased from the Mutant Mouse Resource and Research Center, Hangzhou, Zhejiang province, China (MMRRC_000126-UCD). ROSA26 Cre reporter strain (*R26R-LacZ*) was purchased from the Jackson Laboratory, Bar Harbor, ME, USA (JAX: 009427). The mice were maintained in a temperature-controlled room (22 ± 1 °C) under standard 12-h light/dark cycle, with *ad libitum* access to water and food. The morning that a vaginal plug was detected was considered day 0.5 of pregnancy (E0.5).

X-gal staining

Whole-mount X-gal staining was performed as previously described [41]. Embryos were dissected at defined developmental stages (E10.5, E11.5 and E13.5) and fixed in fresh fix buffer (4% paraformaldehyde (PFA), 2 mM $MgCl_2$, 5 mM EGTA) for 1 h at 4 °C, and then incubated in staining buffer for 2–4 h at 37 °C in the dark. Staining buffer: 2 mM Tris (pH 7.3), 0.1% X-gal, 5 mM potassium ferrocyanide and potassium ferricyanide. X-gal stained sections were counterstained with Nuclear Fast Red.

Cell proliferation and apoptosis assays

Cell proliferation rates were assessed by 5-bromodeoxyuridine (BrdU) labeling. BrdU incorporation assays were performed by intraperitoneal injection of BrdU solution (3 mg per 100 g body weight). Thirty minutes after administeration, the embryonic heads were dissected and fixed overnight in 4% PFA at 4 °C. The collected tissue was then embedded in paraffin and sectioned at 5 µm. The cell proliferation rate was quantified as the percentage of BrdU-positive cells relative to the total number of cells within a defined arbitrary area. Statistical analysis was performed using Student's *t*-test to determine significance. Apoptosis was assayed by TUNEL staining using the *in situ* cell death assay kit following the manufacturer's protocol (Roche, Basel, Switzerland).

Histological analysis and immunofluorescence

Embryos were collected at desired developmental stages and fixed in 4% PFA for 30 min at 4 °C. Samples were then dehydrated through graded alcohols, embedded in paraffin, and sectioned at 7 µm for histological analysis. Serial sections were stained with hematoxylin and eosin according to standard protocol [42]. For immunofluorescence, sections were incubated overnight with primary antibodies diluted with 5% BSA after blocking in 5% BSA. Secondary antibodies conjugated with Alexa Fluor 488 or 594 (1 : 1000; Invitrogen, Carlsbad, CA, USA) diluted in 5% BSA were applied for 30 min in the dark. The primary antibody against BrdU (ab8152; Abcam, Cambridge, UK) was purchased from Abcam.

In situ hybridization

In situ hybridization using whole-mount and section of embryonic samples were performed as previously described, with digoxigenin-labeled antisense RNA probes [43]. For section *in situ* hybridization, embryos were fixed overnight at 4 °C in freshly prepared 4% PFA. Then, embryos were dehydrated through graded alcohols, embedded in paraffin, and sectioned at 12 µm. For whole-mount *in situ* hybridization, samples were fixed in 4% PFA, dehydrated into methanol and bleached with 6% hydrogen peroxide (H_2O_2).

Hybridization signals were visualized with BM Purple alkaline phosphatase Substrate (Roche).

Palatal shelf organ cultures

Bilateral palatal shelves were dissected from E13.5 embryos and placed dorsal side up on a Nuclepore Track-Etch membrane (0.2-μm pore size) within a TROWELL organ culture dish, as previously described [44]. Each pair of palatal shelves was positioned such that the medial edge epithelium (MEE) of each shelf was in contact. After 48 h of culture, explants were harvested and fixed in 4% PFA for histological staining. For *Isl1* overexpression experiments, either the *Isl1* overexpression vector (pCDH-Isl1) or the control vector (pCDH) was transfected into the explants using Lipofectamine 3000 reagent. Following 48 h of incubation in a humidified atmosphere of 5% CO_2 at 37 °C, the explants were collected for RNA extraction and real-time PCR analysis.

In parallel experiments, SHH recombinant protein (100 ng·μL^{-1}) or BSA (100 ng·μL^{-1}) was added to the culture medium to activate the canonical Hedgehog signaling pathway. After 24 h of incubation under the same conditions, explants were harvested for RNA isolation. All experiments were repeated at least three times.

RNA-seq analysis and quantitative real-time PCR

The palatal shelves were dissected from E12.5 embryos and total RNA was extracted as previously described [42]. All the raw data generated from RNA-seq in this work were deposited in BIGD (bigd.big.ac.cn) under the accession number CRA013240. Real-time PCR was performed in triplicate using SsoFast EvaGreen Supermix (Bio-Rad, Hercules, CA, USA). Oligonucleotide primers were designed using PRIMER3 software [45]: *18S* (5′-TAGAGGGACAAGTGGCGTTC, and 5′-CGCTGAGCCAGTCAGTGT), *Shh* (5′-AAAGCTGACCCCTTTAGCCTA and 5′-TGAGTTCCTTAAATCGTTCGGAG), *Isl1 exon2* (5′-CGGCAATCAAATTCACGACC and 5′-TCCCATCCCTAACAAAGCACG), *Isl1* (5′-ATGATGGTGGTTTACAGGCTAAC and 5′-TCGATGCTACTTCACTGCCAG), *Sox2* (5′-CTTTTGTCCGAGACCGAGAAGC and 5′-CCGGGAAGCGTGTACTTATCC), *Foxd2* (5′-ATTTATGAAGAGTCTCCAGACC and 5′-GATGCTCAAACAGAAAAGC), *Foxe1* (5′-ATGACGCGAAACTCCAAAGAGC and 5′-GGCATAGCACACGGTGAAGC), *Ptch1* (5′-AGACTACCCGAATATCCAGCACC and 5′-CCAGTCACTGTCAAATGCATCC). The relative amount of gene transcript was calculated using the $2^{-\Delta\Delta C_T}$ method [46] and normalized to the endogenous *18S* reference gene.

ChIP assay

E13.5 palate samples were collected for chromatin immunoprecipitation (ChIP) analysis. For the binding of ISL1 to the Shh epithelial enhancer sequence (MRCS1), ChIP was carried out using antibody against ISL1 (Abcam) or normal rabbit IgG (Beyotime, Beijing, China). Eluted DNA was used as a template for triplicate quantitative real-time PCR analyses. The specific primers used to amplify the area containing the predicted ISL1 binding site were: B, 5′-CAGACAGATCCACCTGCTGC and 5′-CCTTTTTTGAATCATCACCTGC.

Statistical analyses

All data are presented as means ± SEM. Student's *t*-test was used to test differences between two groups of data. One-way ANOVA and Tukey's test were used to analyze the difference between multiple groups. P values of < 0.05 were regarded as statistically significant.

Acknowledgements

We thank Dr Lin Gan for providing *Isl1*^{fl} and *Isl1*^{lacZ} mice. This work was supported by Zhejiang Provincial Natural Science Foundation of China (LY24C120002 to FL) and National Natural Science Foundation of China (81871166, 81670971 to FL).

Conflict of interest

The authors declare no conflict of interest.

Author contributions

FL contributed to conceptualization, writing—original draft, supervision, project administration, and funding acquisition. JL, HH, and FL contributed to methodology, validation, and formal analysis. CZ, YZ, YQ, RH, and FL contributed to investigation. CZ, YZ, YQ, and RH contributed to data curation. JL, HH, MQ, and FL contributed to writing—review and editing. All authors have read and approved the final version of the manuscript submitted for publication.

Peer review

The peer review history for this article is available at https://www.webofscience.com/api/gateway/wos/peer-review/10.1111/febs.17369.

Data availability statement

All the raw data generated from RNA-seq in this work were deposited in BIGD (bigd.big.ac.cn) under the accession number CRA013240.

References

1 Bush JO & Jiang R (2012) Palatogenesis: morphogenetic and molecular mechanisms of secondary palate development. *Development* **139**, 231–243.
2 Chai Y & Maxson RE Jr (2006) Recent advances in craniofacial morphogenesis. *Dev Dyn* **235**, 2353–2375.
3 Dixon MJ, Marazita ML, Beaty TH & Murray JC (2011) Cleft lip and palate: understanding genetic and environmental influences. *Nat Rev Genet* **12**, 167–178.
4 Gritli-Linde A (2007) Molecular control of secondary palate development. *Dev Biol* **301**, 309–326.
5 Lough KJ, Byrd KM, Spitzer DC & Williams SE (2017) Closing the gap: mouse models to study adhesion in secondary palatogenesis. *J Dent Res* **96**, 1210–1220.
6 Parada C & Chai Y (2012) Roles of BMP signaling pathway in lip and palate development. *Front Oral Biol* **16**, 60–70.
7 Smith TM, Lozanoff S, Iyyanar PP & Nazarali AJ (2012) Molecular signaling along the anterior-posterior axis of early palate development. *Front Physiol* **3**, 488.
8 Iwata J, Tung L, Urata M, Hacia JG, Pelikan R, Suzuki A, Ramenzoni L, Chaudhry O, Parada C, Sanchez-Lara PA *et al.* (2012) Fibroblast growth factor 9 (FGF9)-pituitary homeobox 2 (PITX2) pathway mediates transforming growth factor beta (TGFbeta) signaling to regulate cell proliferation in palatal mesenchyme during mouse palatogenesis. *J Biol Chem* **287**, 2353–2363.
9 Rice R, Connor E & Rice DP (2006) Expression patterns of hedgehog signalling pathway members during mouse palate development. *Gene Expr Patterns* **6**, 206–212.
10 Lan Y, Xu JY & Jiang RL (2015) Cellular and molecular mechanisms of palatogenesis. *Curr Top Dev Biol* **115**, 59–84.
11 Lee JM, Miyazawa S, Shin JO, Kwon HJ, Kang DW, Choi BJ, Lee JH, Kondo S, Cho SW & Jung HS (2011) Shh signaling is essential for rugae morphogenesis in mice. *Histochem Cell Biol* **136**, 663–675.
12 Pantalacci S, Prochazka J, Martin A, Rothova M, Lambert A, Bernard L, Charles C, Viriot L, Peterkova R & Laudet V (2008) Patterning of palatal rugae through sequential addition reveals an anterior/posterior boundary in palatal development. *BMC Dev Biol* **8**, 116.
13 Welsh IC & O'Brien TP (2009) Signaling integration in the rugae growth zone directs sequential SHH signaling center formation during the rostral outgrowth of the palate. *Dev Biol* **336**, 53–67.
14 Lan Y & Jiang R (2009) Sonic hedgehog signaling regulates reciprocal epithelial-mesenchymal interactions controlling palatal outgrowth. *Development* **136**, 1387–1396.
15 Moreno LM, Mansilla MA, Bullard SA, Cooper ME, Busch TD, Machida J, Johnson MK, Brauer D, Krahn K, Daack-Hirsch S *et al.* (2009) FOXE1 association with both isolated cleft lip with or without cleft palate, and isolated cleft palate. *Hum Mol Genet* **18**, 4879–4896.
16 Sweat YY, Sweat M, Yu W, Sanz-Navarro M, Zhang L, Sun Z, Eliason S, Klein OD, Michon F, Chen Z *et al.* (2020) Sox2 controls periderm and rugae development to inhibit oral adhesions. *J Dent Res* **99**, 1397–1405.
17 Venza I, Visalli M, Parrillo L, De Felice M, Teti D & Venza M (2011) MSX1 and TGF-beta3 are novel target genes functionally regulated by FOXE1. *Hum Mol Genet* **20**, 1016–1025.
18 Yang L, Cai CL, Lin LZ, Qyang YB, Chung C, Monteiro RM, Mummery CL, Fishman GI, Cogen A & Evans S (2006) Isl1Cre reveals a common Bmp pathway in heart and limb development. *Development* **133**, 1575–1585.
19 Zhang W, Yu JJ, Fu GQ, Li JY, Huang HR, Liu J, Yu DL, Qiu MS & Li FX (2022) ISL1/SHH/CXCL12 signaling regulates myogenic cell migration during mouse tongue development. *Development* **149**, dev200788.
20 Mitsiadis TA, Angeli I, James C, Lendahl U & Sharpe PT (2003) Role of Islet1 in the patterning of murine dentition. *Development* **130**, 4451–4460.
21 Li FX, Fu GQ, Liu Y, Miao XP, Li Y, Yang XQ, Zhang XY, Yu DL, Gan L, Qiu MS *et al.* (2017) ISLET1-dependent beta-catenin/hedgehog signaling is required for outgrowth of the lower jaw. *Mol Cell Biol* **37**, e00590-16.
22 Attanasio C, Nord AS, Zhu Y, Blow MJ, Li Z, Liberton DK, Morrison H, Plajzer-Frick I, Holt A, Hosseini R *et al.* (2013) Fine tuning of craniofacial morphology by distant-acting enhancers. *Science* **342**, 1241006.
23 Sagai T, Amano T, Tamura M, Mizushina Y, Sumiyama K & Shiroishi T (2009) A cluster of three long-range enhancers directs regional Shh expression in the epithelial linings. *Development* **136**, 1665–1674.
24 Varjosalo M & Taipale J (2008) Hedgehog: functions and mechanisms. *Genes Dev* **22**, 2454–2472.
25 Baek JA, Lan Y, Liu H, Maltby KM, Mishina Y & Jiang RL (2011) Bmpr1a signaling plays critical roles in palatal shelf growth and palatal bone formation. *Dev Biol* **350**, 520–531.
26 Hosokawa R, Deng XM, Takamori K, Xu X, Urata M, Bringas P & Chai Y (2009) Epithelial-specific requirement of FGFR2 signaling during tooth and palate development. *J Exp Zool B Mol Dev Evol* **312b**, 343–350.
27 Juriloff DM & Harris MJ (2008) Mouse genetic models of cleft lip with or without cleft palate. *Birth Defects Res A Clin Mol Teratol* **82**, 63–77.
28 Riley BM, Mansilla MA, Ma J, Daack-Hirsch S, Maher BS, Raffensperger LM, Russo ET, Vieira AR,

Dodé C, Mohammadi M *et al*. (2007) Impaired FGF signaling contributes to cleft lip and palate. *Proc Natl Acad Sci USA* **104**, 4512–4517.
29 Yu HM, Smallwood PM, Wang YS, Vidaltamayo R, Reed R & Nathans J (2010) Frizzled 1 and frizzled 2 genes function in palate, ventricular septum and neural tube closure: general implications for tissue fusion processes. *Development* **137**, 3707–3717.
30 Li C, Lan Y & Jiang R (2017) Molecular and cellular mechanisms of palate development. *J Dent Res* **96**, 1184–1191.
31 Xu JY, Liu H, Lan Y, Aronow BJ, Kalinichenko VV & Jiang RL (2016) A Shh-Foxf-Fgf18-Shh molecular circuit regulating palate development. *PLoS Genet* **12**, e1005769.
32 Zhang Z, Song Y, Zhao X, Zhang X, Fermin C & Chen Y (2002) Rescue of cleft palate in Msx1-deficient mice by transgenic Bmp4 reveals a network of BMP and Shh signaling in the regulation of mammalian palatogenesis. *Development* **129**, 4135–4146.
33 Su TT, Liu H, Zhang D, Xu GJ, Liu JL, Evans SM, Pan JR & Cui S (2019) LIM homeodomain transcription factor Isl1 affects urethral epithelium differentiation and apoptosis via. *Cell Death Dis* **10**, 713.
34 Amano K, Okuzaki D, Aikawa T & Kogo M (2020) Indian hedgehog in craniofacial neural crest cells links to skeletal malocclusion by regulating associated cartilage formation and gene expression. *FASEB J* **34**, 6791–6807.
35 Pathi S, Pagan-Westphal S, Baker DP, Garber EA, Rayhorn P, Bumcrot D, Tabin CJ, Pepinsky RB & Williams KP (2001) Comparative biological responses to human Sonic, Indian, and Desert hedgehog. *Mech Dev* **106**, 107–117.
36 Li JY, Yuan Y, He JZ, Feng JF, Han X, Jing JJ, Ho T, Xu J & Chai Y (2018) Constitutive activation of hedgehog signaling adversely affects epithelial cell fate during palatal fusion. *Dev Biol* **441**, 191–203.
37 Brancaccio A, Minichiello A, Grachtchouk M, Antonini D, Sheng H, Parlato R, Dathan N, Dlugosz AA & Missero C (2004) Requirement of the forkhead gene Foxe1, a target of sonic hedgehog signaling, in hair follicle morphogenesis. *Hum Mol Genet* **13**, 2595–2606.
38 Jeong J, Mao J, Tenzen T, Kottmann AH & McMahon AP (2004) Hedgehog signaling in the neural crest cells regulates the patterning and growth of facial primordia. *Genes Dev* **18**, 937–951.
39 Pan L, Deng M, Xie X & Gan L (2008) ISL1 and BRN3B co-regulate the differentiation of murine retinal ganglion cells. *Development* **135**, 1981–1990.
40 Yang L, Gu SP, Ye WD, Song YG & Chen YP (2016) Augmented Indian hedgehog signaling in cranial neural crest cells leads to craniofacial abnormalities and dysplastic temporomandibular joint in mice. *Cell Tissue Res* **364**, 105–115.
41 Li JY, Cui Y, Xu J, Wang QH, Yang XQ, Li Y, Zhang XY, Qiu MS, Zhang Z & Zhang ZY (2017) Suppressor of fused restraint of hedgehog activity level iscritical for osteogenic proliferation and differentiation during calvarial bone development. *J Biol Chem* **292**, 15814–15825.
42 Chen LY, Zhang W, Huang RQ, Miao XP, Li JY, Yu DL, Li Y, Hsu W, Qiu MS, Zhang ZY *et al*. (2021) The function of Wls in ovarian development. *Mol Cell Endocrinol* **522**, 111142.
43 Li J, Xu J, Cui Y, Wang L, Wang B, Wang Q, Zhang X, Qiu M & Zhang Z (2019) Mesenchymal Sufu regulates development of mandibular molar via Shh signaling. *J Dent Res* **98**, 1348–1356.
44 Huang RQ, Zhang CJ, Zheng YT, Zhang W, Huang HR, Qiu MS, Li JY & Li FX (2023) ISL1 regulates lung branching morphogenesis via Shh signaling pathway. *J Biol Chem* **299**, 105034.
45 Rozen S & Skaletsky H (2000) Primer3 on the WWW for general users and for biologist programmers. *Methods Mol Biol* **132**, 365–386.
46 Livak KJ & Schmittgen TD (2001) Analysis of relative gene expression data using real-time quantitative PCR and the 2(-Delta Delta C(T)) method. *Methods* **25**, 402–408.